УДК 539.1.08+539.128.2

MOMENTUM RECONSTRUCTION PROCEDURE FOR A NONFOCUSING SPECTROMETER WITH WIDE-APERTURE ANALYZING MAGNET AND NONUNIFORM FIELD

L.S.Azhgirey[1], *W.Augustyniak*[2], *L.Farhi*[3,4], *R.A.Kunne*[3], *L.V.Malinina*[1], *E.A.Strokovsky*[1]

The SPES-4 spectrometer at SATURNE II has recently been equipped with a detection system working in coincidence with it. This system uses a wide-aperture dipole magnet. In the paper a method is described to determine the momentum vector and interaction vertex of the detected charged particle from its trajectory parameters measured outside the inhomogeneous field of the magnet. The feature of the set-up is that all detectors are placed outside the dipole field, while the target is inside the ~1 T field and the incoming track is not measured. The feature of the method is that it is simple and fast, while it uses only the straight line part of the particle trajectory, which can be measured with sufficient accuracy.

The investigation has been performed at the Laboratory of High Energies, JINR.

Процедура восстановления импульса для нефокусирующего спектрометра с широкоапертурным анализирующим магнитом и неоднородным магнитным полем

Л.С.Ажгирей и др.

SPES-4 спектрометр на SATURNE II был недавно оснащен детектирующей системой, работающей в совпадении с ним. Эта система включает в себя широкоапертурный магнит. В статье описывается метод определения импульса и координат вершины взаимодействия заряженной частицы по параметрам траектории, измеренным вне неоднородного магнитного поля этого магнита. Особенность расположения детекторов заключается в том, что все они находятся за областью поля, тогда как мишень находится внутри области с напряженностью поля ~1 Т, а параметры входящего в мишень трека не измеряются. Достоинства метода в его простоте и быстроте,

[1]Joint Institute for Nuclear Research, 141980 Dubna, Russia
[2]IPN Orsay, CNRS/IN2P3, France
[3]Soltan Institute for Nuclear Studies, 00-681 Warsaw, Poland
[4]Current address: CEA/DAPNIA/SPhN, CE-Saclay, France

хотя используется только прямолинейная часть траектории частицы, которая может быть измерена с достаточной точностью.

Работа выполнена в Лаборатории высоких энергий ОИЯИ.

1. INTRODUCTION

Several years ago a strong isoscalar excitation of the proton in the region of the Roper resonance $N^*(1440$ MeV) was measured at SATURNE (see Ref.1) in the inclusive $p(\alpha, \alpha')X$ reaction using the SPES-4 spectrometer. With the goal of an exclusive study of this excitation in the interactions of α particles and polarized deuterons with protons, the SPES-4 spectrometer at SATURNE II has been equipped with a detection system working in coincidence with it. This system includes a wide-aperture dipole magnet, TETHYS, a hydrogen target located between the magnet poles in the region of the magnetic field, proportional and drift chambers to measure particle coordinates outside the inhomogenous magnetic field of TETHYS. In this paper we describe a simple and fast procedure that uses only the straight line parts of particle trajectories to reconstruct the values of momenta and angles of emission from the target of the particles detected. Recently the same problem has been considered in Ref.2 for a selected set of parameters defining the trajectories. The method proposed in this paper seems to be more general.

The paper is organized as follows. The brief description of the experimental set-up, SPES-4π, is given in Sec. 2. In Sec. 3 we present the results of measurements of the magnetic field of the Tethys magnet. The description of the method of momentum reconstruction of particles detected by the spectrometer is given in Sec. 4. The application of this method to the experimental data obtained in $p(d, d')X_{charged}$ experiment with SPES-4π is illustrated in Sec. 5.

2. DESCRIPTION OF SPES-4π SET-UP

The scheme of SPES-4π set-up used in a series of experiments at SATURNE II beams is shown in Fig.1.

It consists of a large acceptance nonfocusing magnetic spectrometer ("FS+LS") in combination with the high resolution focusing magnetic spectrometer SPES-4 [3]. The particles of high momenta (in this experiment the d') were detected in SPES-4, while the secondary charged particles of low momenta (protons, pions, deuterons) were detected in the nonfocusing spectrometer "FS+LS". In the typical experiment with SPES-4π, reactions of the type $b + t \to s + c_1 + c_2 + ... + X$ were studied. Here b is the beam particle, t is the target particle, s is the scattered particle detected in SPES-4 and c_i $(i = 1, 2, ..)$ is a charged particle detected by the "FS+LS" spectrometer.

SPES-4 spectrometer is $\sim$33 meter long and consists of two almost identical bends, made of four identical dipoles, six quadropoles and a correcting sextupole; two scintillation hodoscopes (I and F) placed at the intermediate focus (I, after the first bend) and in the final focus (F), 2 cm thick scintillators (ΔE-detector) placed after the hodoscope of the final focus in order to measure ionization losses of the detected particles and two drift chambers (with four wire planes each) before the F-hodoscope. These chambers provided

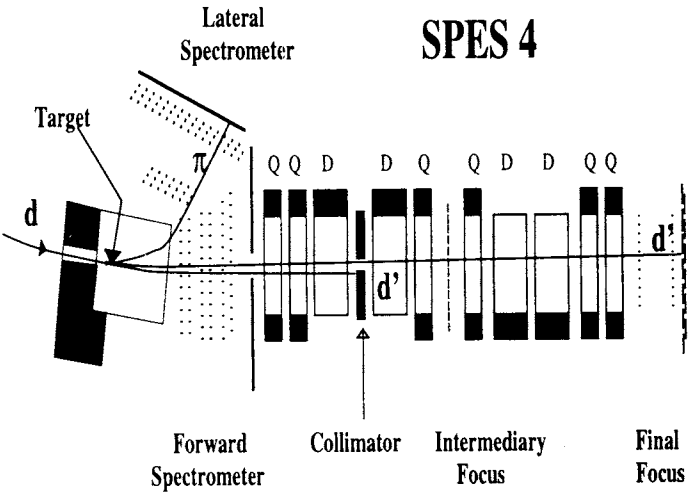

Fig. 1. Schematic view of SPES-4π set-up

the momentum resolution of $\sim$0.1% and the angular resolution of $\sim$1 mrad. The acceptance of the spectrometer is $\sim 2 \times 10^{-4}$ sr. Particles are identified by the values of p/z, time of flight and the energy lossed in the ΔE-detector*.

In the past, SPES-4 has been used as a stand–alone spectrometer. When used in coincidence with the detection system partially surrounding the target, care has to be taken that the through–going beam is trapped correctly. In practice this means that the direction of the outgoing beam and the particle detected in SPES-4 are separated not more than a degree at the entrance of SPES-4. Therefore in this experiment the outgoing beam was trapped after the first dipole of SPES-4 by 50 cm thick lead collimator.

The "FS+LS" spectrometer consists of two arms: the lateral arm (LS) and the forward arm (FS), each equipped with a scintillator hodoscope used for trigger and particle identification, as well as coordinate detectors (the drift and proportional multiwire chambers).

The lateral arm (LS) has two multiwire proportional chambers, each with three planes with a wire spacing of 2.5 and 4.7 mm, respectively.

The forward arm (FS) (described in detail in Ref.2) consists of six chambers with a total of twelve planes of drift cells; the coordinate resolution of these chambers is $\sim$ 0.3 mm in the "drift mode"; when only a number of active wire is used for tracking (the "proportional chamber mode"), the resolution is 1.2 mm because the distance of the two neighbourgh drift cells is 4.33 mm.

The forward scattered particles and the unscattered beam passed free through the hole in each of the forward arm chambers into entrance of SPES-4.

Particles detected in the FS or LS arms are identified by the values of p/z, time of flight and the energy lossed in the hodoscopes.

Both arms are located in the fringe field region of the dipole magnet TETHYS. Its pole face has the shape of a square with a side of 100 cm; the pole aperture is 50 cm. The magnet

*Here p is the momentum of the detected particle; z, its charge.

is oriented with its iron yoke in the direction of the incoming beam (with momentum of 3.73 GeV/c) which passed through the hole (of 20 cm width and 10 cm height) in the yoke to the target (6 cm of liquid hydrogen) placed at a distance of $\sim$ 25 cm downstream from the yoke.

Events were selected by coincidence between signal from SPES-4 (which corresponds to coincidence between counters of I and F hodoscopes of SPES-4) and the logical sum of signals from hodoscopes of FS and LS arms.

3. MAGNETIC FIELD OF TETHYS

The vertical component of the magnetic field was measured at three field strengths (6, 9, 12 kG), both in the median plane and in the plane 15 cm above the median plane in a rectangular grid of 98 by 129 points, with a spacing of 2 cm.

The field in the region of the beam was measured over the whole distance from the entry hole in the magnet's yoke up to the entrance of SPES-4, in 5 cm steps. From the measured field values, a 3-dimensional field map was constructed using an algorithm taken from the ZGOUBI tracking simulation (Ref.4, see Fig. 2). First, the median plane field was extrapolated to a surface of 4×3.7 m^2.The B_Y component and the partial derivatives with respect to X and Z were interpolated by polynomial fits. Next, all three field components outside the median plane were obtained by a Taylor series development of the Maxwell equations. The second order of the Taylor series development was used.

The out-of-plane measurements were used to check the consistency of this procedure. It was found that the differences between the calculated and the measured field components are in absolute value less than 100 Gauss in each point.

4. METHOD OF MOMENTUM RECONSTRUCTION

To determine the momentum and the angles of the particle emitted from the target when its trajectory parameters are measured by the drift chambers, we have used a method where explicit functions are constructed, which give these values in terms of the measured quantities (see Refs.5).

The realization of the method has two steps:

— "Teaching" the code: generate trial tracks and find necessary coefficients.

— Use the "educated" code with the found coefficients in order to get vector of the momentum using coordinates in the reference planes:

1. Estimate the momentum vector in the Homogenous Field Approximation (HFA);
2. Correct the HFA result using the coefficients.

In this method a number of trial trajectories have to be computed, which represent the space of possible trajectories in the set-up. These trajectories are used as a basis to obtain the explicit reconstruction functions. In the following we choose a reference frame with the z axis along the TETHYS magnet, from the target to the forward hodoscope and the y axis along the main component of the magnetic field.

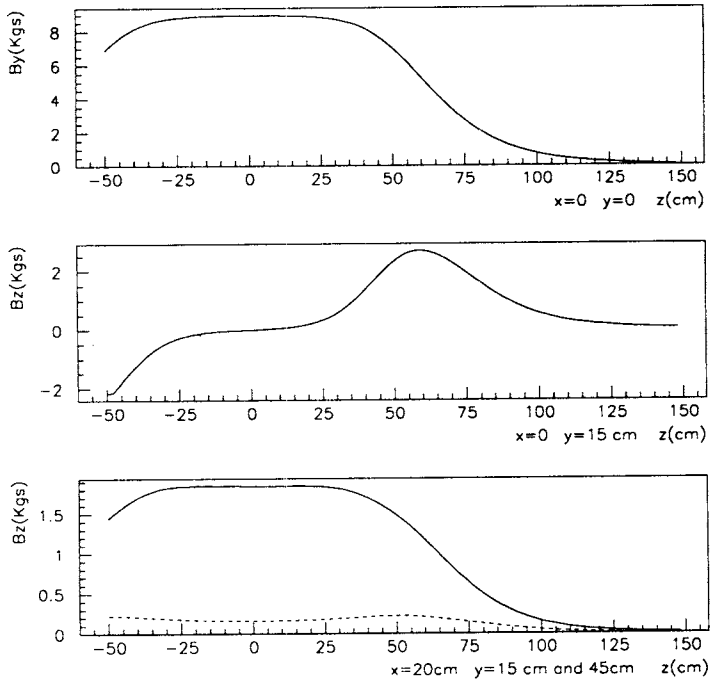

Fig. 2. Magnetic field components B_y, B_z, B_x for 9 KGs field. The broken line corresponds to $y = 15$ cm; the full line corresponds to $y = 45$ cm

The initial conditions for each trajectory can be described by a 4-dimensional vector $\vec{P}$ with components

$$\begin{aligned} P_1 &= 1/(pc), \\ P_2 = \tan\theta_x &= \tan\vartheta\,\cos\varphi, \\ P_3 = \sin\theta_y &= \sin\vartheta\,\sin\varphi, \\ P_4 &= z_{targ}, \end{aligned} \tag{1}$$

where p is the momentum of a charged particle; z_{targ} is the z-coordinate in the target; θ_x and θ_y are the emission angles in the horizontal and vertical planes, respectively; and ϑ, φ are the angles in the spherical coordinate frame. With these initial conditions and with use of the magnetic field map, each trajectory can be computed.

The lower and upper limits of the interval, where each variable P_1, P_2, P_3, P_4 run, were chosen in such a way that the full acceptance of the FS was covered. Note that in general case the particle trajectory has five degrees of freedom in six-dimensional phase space and therefore to describe the trajectory one needs five independent variables.

In our case the width of the beam is small with respect to the resolution on the vertex coordinates that we may expect. Therefore we assume that four independent variables are sufficient to describe the particle path. For each coordinate interval we have taken a grid of discrete, equal length, steps. The number of steps N_1, N_2, N_3, N_4 were chosen in such a way that the required accuracy in the final function can be achieved. Next, we followed the

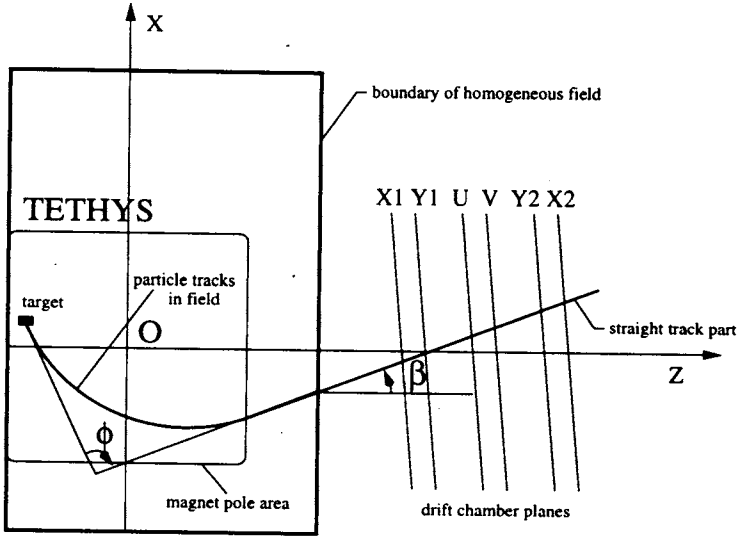

Fig. 3. Definition of the coordinate system

trajectories through the magnetic field for all possible combinations of these variables, a total of $N = N_1 \cdot N_2 \cdot N_3 \cdot N_4$ trajectories. For each trajectory we determined a 4-dimensional vector $\vec{X}$ of coordinates

$$X_1 = x_1, \quad X_2 = x_2, \quad X_3 = y_1, \quad X_4 = y_2, \tag{2}$$

where x_1, y_1 and x_2, y_2 are the coordinates of crossing by a particle the first and the last planes of drift chambers, respectively.

To be able to reconstruct the momentum variables, we first calculate a vector $\vec{P}'$ under the assumption that the field is constant inside the region indicated by the solid line in Fig. 3 and zero outside. In this Homogenous Field Approximation (HFA) the components of $\vec{P}'$ can be related to coordinates (x, z) of the point, where the particle crossed the boundary of the homogenous field at an angle of β:

$$\begin{aligned} \sin\theta_x &= \frac{2\,L\,x\,\cos\beta - (L^2 - x^2)\,\sin\beta}{L^2 + x^2}, \\ (pc)_{xz} &= \frac{C}{(\cos\theta_x + \cos\beta)\,\tan\frac{\phi}{2}}, \\ (pc)_y &= (pc)_{xz}\,\tan\theta_y, \\ L &= z - z_{targ} \end{aligned} \tag{3}$$

Here $(pc)_{xz}$ and $(pc)_y$ are the components of momentum in the xOz plane and along the y axis, respectively. C is a constant proportional to the strength of the magnetic field. $\phi = \beta - \theta_x$ is the angle of deflection of a charged particle in the field. Outside the magnetic field the particle movement is assumed rectilinear; therefore the coordinates x, z, and angle β can be readily related to the coordinates of the particle when crossing the drift chamber planes.

To relate estimation $\vec{P}'$ of the momentum vector with the real one $\vec{P}$, we proceed as follows. First we calculated the mean values

$$< X_j >= \frac{1}{N} \sum_{k=1}^{N} X_{kj} \tag{4}$$

for each component j, and the correlation matrix

$$A_{ij} = \sum_{k=1}^{N} (X_{ki} - < X_i >)(X_{kj} - < X_j >). \tag{5}$$

If the eigenvectors of the correlation matrix are $\vec{w}_l$ $(l = 1, ..., 4)$, one can define a new set of coordinates $\vec{\xi}$ as the component of the observable $\vec{X}$ in the coordinate system defined by the $\vec{w}_l$:

$$\xi_l = \sum_i w_{il} X_i, \tag{6}$$

where w_{il} is the i-th component of the eigenvector corresponding to the l-th eigenvalue. This procedure reduces the region of interest. For the matrix of the ratios $Q_{ik} = P_{ik}/P'_{ik}$ $(i = 1, ..., 4)$ we determine in a similar way the eigenvectors $\vec{v}_j$ of the correlation matrix

$$B_{ij} = \sum_{k=1}^{N} (Q_{ki} - < Q_i >)(Q_{kj} - < Q_j >) \tag{7}$$

and define variables

$$\zeta_j = \sum_i v_{ij} Q_i. \tag{8}$$

For each component of $\vec{\zeta}$ we can make a 4-dimensional fit, using $\vec{\xi}$ as variables, thus determining 4 sets of coefficients $\vec{c}_j$,

$$\zeta_j = \sum_i c_{ij} f_i(\vec{\xi}), \tag{9}$$

where $f_i(\vec{\xi})$ is some function of $\vec{\xi}$, for instance, a polynomial. The coefficients $\vec{c}_j$ can be computed making use of the Gram-Schmidt orthogonalization process [6].

The procedure is now complete. For actual data one needs to calculate the HFA vector $\vec{P}'$ from a set of chamber coordinates $\vec{X}$ according to (3). The vector $\vec{\xi}$ is defined by the transformation (6), while $\vec{\zeta}$ follows from the coefficients $\vec{c}_j$ and equation (9). Finally, the components of the momentum vector $\vec{P}$ are calculated from

$$P_i = P'_i \sum_j v_{ij} \zeta_j. \tag{10}$$

5. APPLICATION

The above general approach developped by Wind in Refs.5 has been applied to Monte-Carlo simulated trajectories and to the real data from the reaction $d + p \to p + d$. The data from this reaction has been taken in the $p(d, d')X$ experiment using the SPES-4π spectrometer and the polarized deuteron beam of Saturne II.

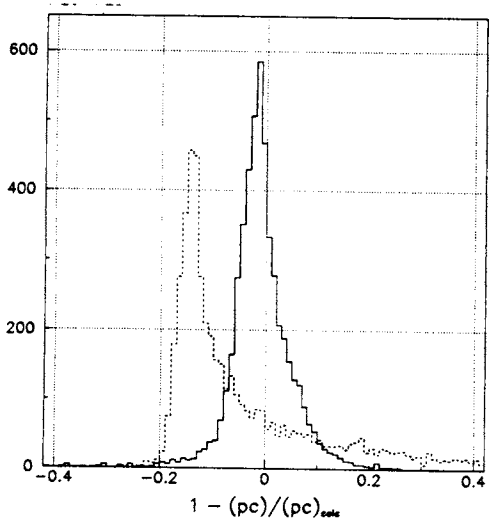

Fig. 4. Difference between the starting and restored momenta. The broken line corresponds to HFA method; the full line corresponds to the method of coefficients

5.1. Application of the Method for Simulated Events. Particles detected in FS-spectrometer (π, protons, deuterons) have typical momenta in the region from ~0.4 to 3 GeV/c. This range was divided in two parts: from 0.4 to 0.9 GeV/c and from 0.75 to 3 GeV/c. The coefficients $\vec{c}_j$ were determined for each of the parts separately. Furthermore, since the magnetic field was highly symmetric about the horizontal plane, the interval of P_3 was considered for one half of the magnetic field only. Eight equidistantly spaced points were chosen in each of the intervals of P_1 and P_2, 4 points in the interval of P_3 and 6 points along the 6 cm long target. The trajectories through the magnetic field were computed for both sets of these 1536 points and 30 coefficients $\vec{c}_j$ for each P_k were determined to calculate $\vec{P}$ from actual observations, as described above.

One of the important factors which limits the momentum resolution of the "FS+LS" spectrometer is the length of the target.

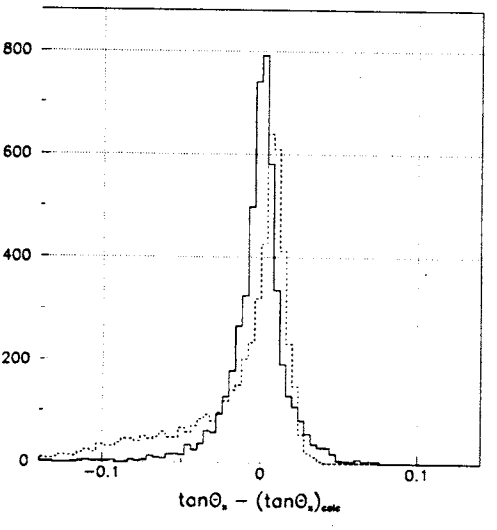

Fig. 5. Difference of starting and restored emission angles $\sin(\theta_y)$: The broken line corresponds to HFA method; the full line corresponds to the method of coefficients

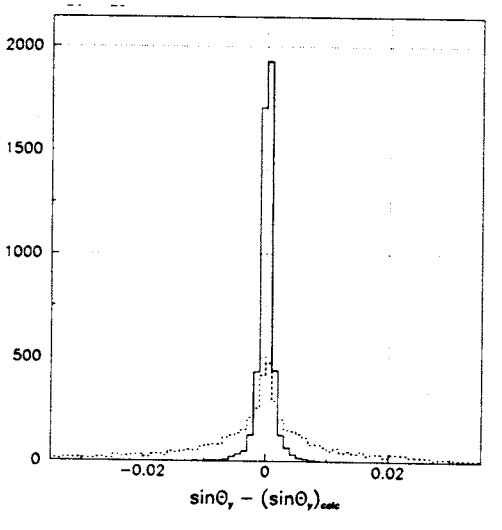

Fig. 6. Difference between the starting and restored momenta. The broken line corresponds to HFA method; the full line corresponds to the method of coefficients

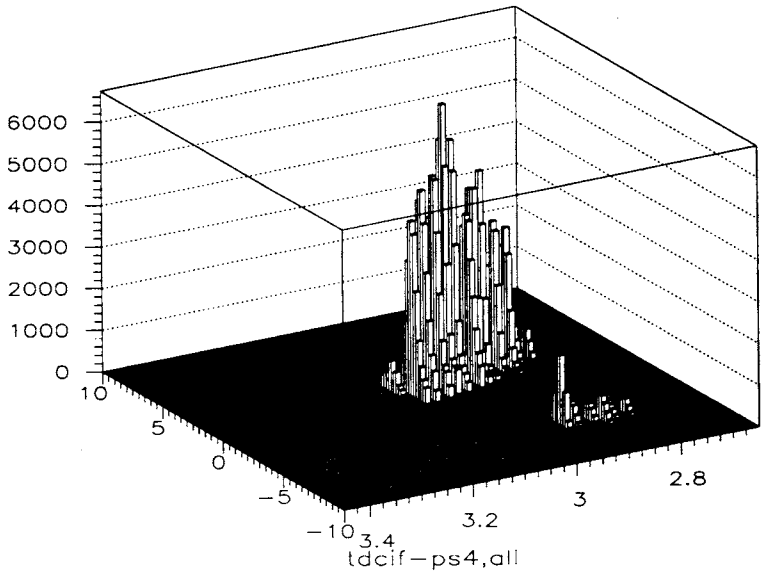

Fig. 7. Event distribution on the plot of "momentum in SPES-4" (GeV/c) – "time of flight in SPES-4" (ns). Deuterons in SPES-4 from inelasic $p(d,d')$ reaction (the big "mountain"), protons from $p(d,p)d$ (the small peak), and $p(d,p)pn$ (the tail of the small peak) reactions are separated clearly

As a test, the accuracy of the method was compared under two conditions: 1) the point of interaction in the target is known and 2) there is uncertainty in this variable.

The accuracy has been estimated by generating tracks with random values $P_1, ..., P_4$, uniformly distributed in their respective ranges, performing tracking, calculating the coordinates $X_1, ..., X_4$ and then using these X_i to determine the P'_k by means of the known coefficients $\vec{c}_j$. The distributions of the differences of calculated values $(pc), \tan\theta_x, \sin\theta_y$ from respective starting ones are shown in Figs. 4—6, where:

– the broken lines correspond to the HFA vector P'_k,

– the full lines correspond to the reconstructed vector P_k.

The RMS deviations of these differences for these two variants in comparison with the homogeneous field approximation (HFA) are given in the Table.

Table. RMS deviations of differences between initial and reconstructed momenta and emission angles

calculation:	HFA	complete	z_{targ} known
$\Delta p/p$	0.222	0.0591	0.0038
$\Delta\theta_x$	0.035	0.0197	0.0064
$\Delta\theta_y$	0.016	0.0014	0.0006

It is seen from Figs. 4—6 and the Table that the method used for evaluating momenta and emission angles of particles gives better results than HFA. The relatively moderate accuracy of the reconstruction of momentum and emission angles of particle detected stems from the

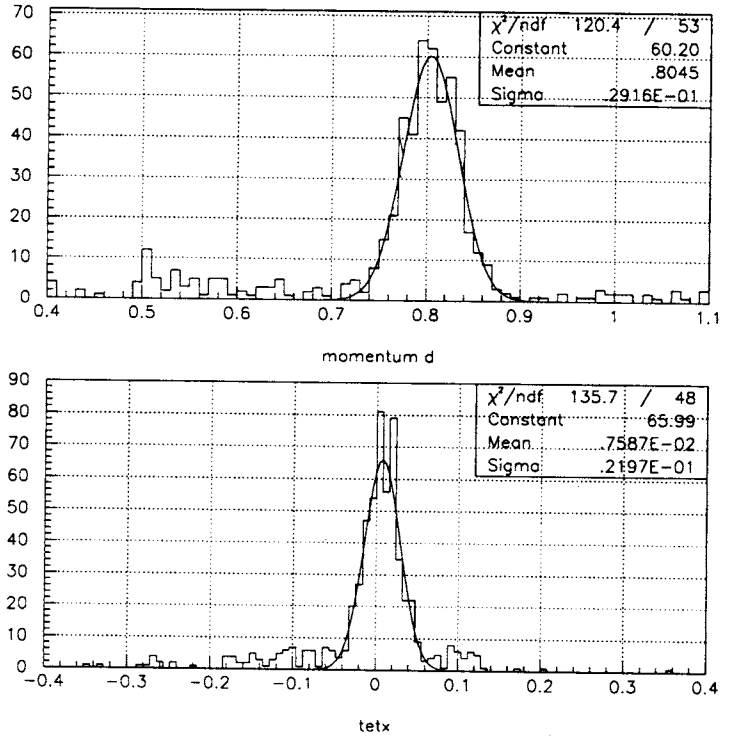

Fig. 8. Momentum and the emission angle of deuterons from $dp \to pd$ at 180° at c.m.; here the "proportional chamber mode" was used for tracking

poor knowledge of the z-vertex coordinate of the track of the particle emitted from the target. Indeed, the computation with a known value of z-coordinate yields a large gain in accuracy of the reconstruction in comparison with the HFA, as can be seen from the Table.

5.2. Application of the Method to Real Events. The method has been applied to the real data from semi-exclusive $p(d,d')X$ experiment using the SPES-4π set-up. Detected events come mostly from two reactions (Fig.7): the inelasic $p(d,d')X_{ch}$ (deuterons were detected in SPES-4) and elastic backward (in c.m.) $p(d,p)d$ scattering. The latter reaction was unambigiously identified by detecting recoil proton in SPES-4 (with momentum of 2.93 GeV/c) in coincidence with scattered deuteron in FS (with momentum of $\sim$ 0.8 GeV/c).

The momentum reconstruction procedure has been applied to the reconstruction of the momentum of the slow deuterons from this reaction.

The reconstructed scattering angle (θ_x) and momentum of deuterons are shown in Fig.8. It is seen that the reconstructed momentum $P_d = 0.805 \pm 0.029$ (GeV/c) and the scattering angle $\theta_x = 0.008 \pm 0.022$ (rad) are in good agreement with kinematical calculations for $p + d \to d + p$ at the beam momentum of 3.73 GeV/c. The widths of the momentum and the angular distributions are determined by the uncertainty in the z coordinate of the interaction point, multiple Coulomb scattering in air and in the material of the drift chambers, the accuracy of measurements of the coordinates and the accuracy of the measurements and extrapolation procedures of the magnetic field map.

6. CONCLUSION

The method used for evaluating momenta and emission angles of particles gives considerably better results than HFA, although the z coordinate of the interaction vertex is known poorly (with accuracy of $60/\sqrt{12} = 17.3$ mm).

The application of the method to real events demonstrates its feasibility. The Monte-Carlo description of the set-up and the available field map provide good tool for estimations of the systematic errors of the momentum reconstruction method used.

References

1. Morsch H.P. et al. — Phys. Rev. Lett., 1992, v.69, p.1336.

2. Alkhazov G.D., Kravtsov A.V., Prokofiev A.N. — Preprint PNPI EP-32-1998, No. 2246, PNPI, Gatchina, 1998.

3. Arvieux J. et al. — Phys. Rev. Lett., 1983, v.50, p.19; Arvieux J. et al. — Nucl. Phys., 1984, v.A431, p.1613; Boudard A. — Thesis, CEA-N-2386, 1984 (unpublished).

4. Meot F., Valero S. — Saturne note LNS/GT/93-12 "Zgoubi Users Guide Ver3", LNS, 1993.

5. Lechanoine C., Martin M., Wind H. — NIM, 1969, v.69, p.122; Wind H. — CERN computer and data proceeding school, 1972, p.53.

6. Rice G.R. — Math. Comput., 1966, v.20, No. 94, p.325.

Received on March 1, 1999.